Perspectives for next beta-decay and delayed-neutron data table

Futoshi Minato
Kyushu University

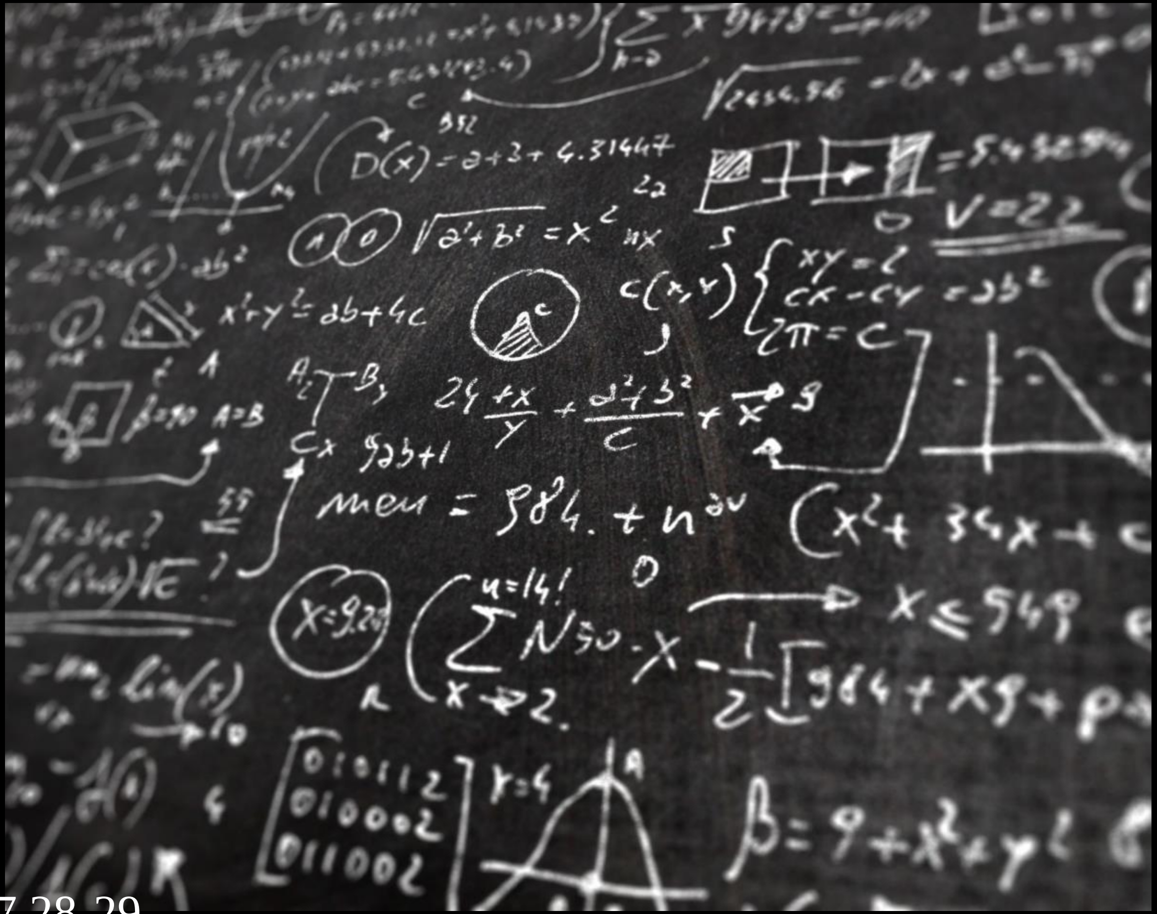

Contents
1) Background
2) Purpose & Strategy
3) Result
4) Summary

Structure of the neutron-rich matter revealed by beta decay 2024 07.28-29

BACKGOUND

JAEA Chart of the Nuclides (2014)

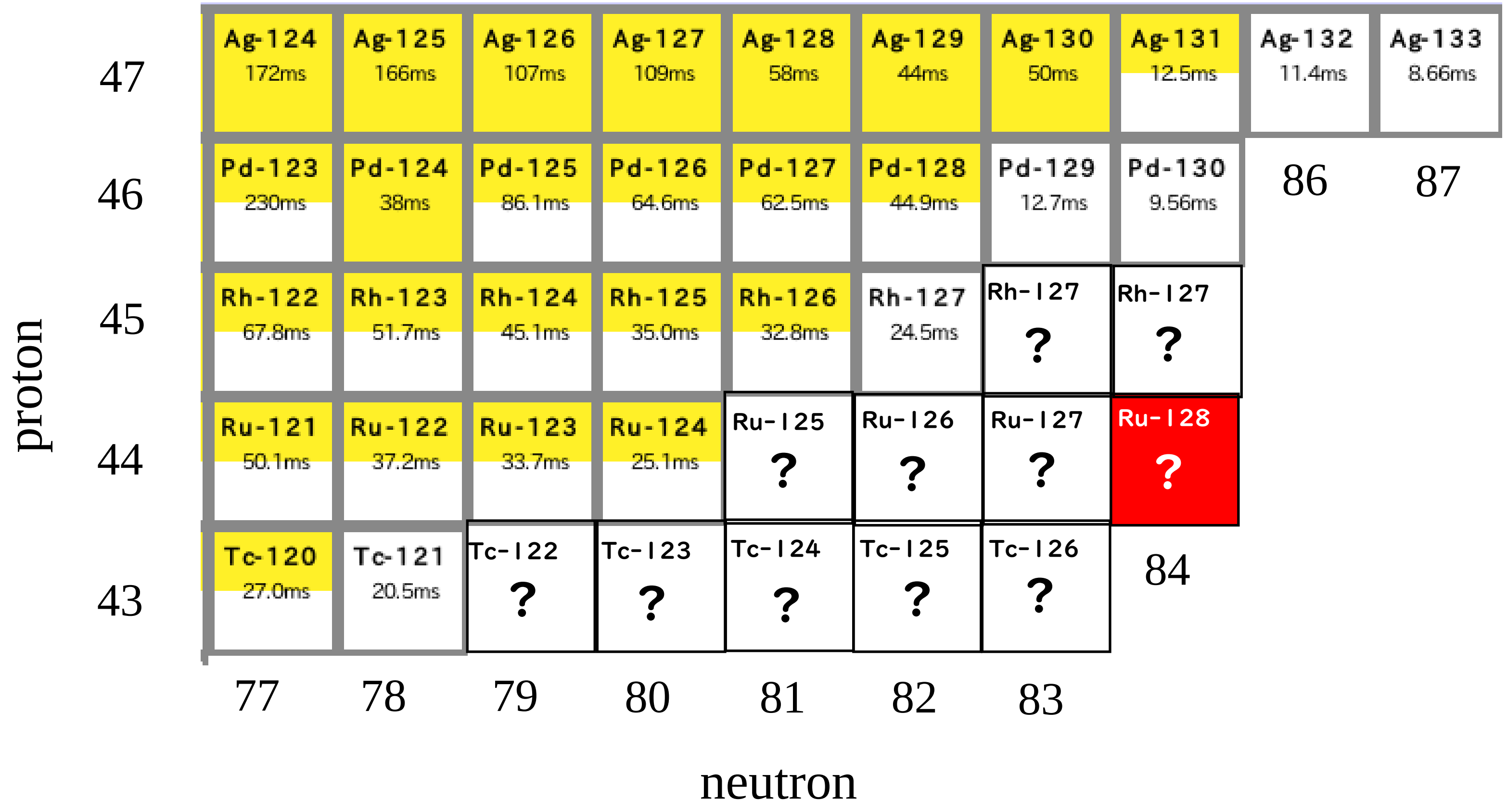

	77	78	79	80	81	82	83	84	86	87
47	Ag-124 172ms	Ag-125 166ms	Ag-126 107ms	Ag-127 109ms	Ag-128 58ms	Ag-129 44ms	Ag-130 50ms	Ag-131 12.5ms	Ag-132 11.4ms	Ag-133 8.66ms
46	Pd-123 230ms	Pd-124 38ms	Pd-125 86.1ms	Pd-126 64.6ms	Pd-127 62.5ms	Pd-128 44.9ms	Pd-129 12.7ms	Pd-130 9.56ms		
45	Rh-122 67.8ms	Rh-123 51.7ms	Rh-124 45.1ms	Rh-125 35.0ms	Rh-126 32.8ms	Rh-127 24.5ms	Rh-127 ?	Rh-127 ?		
44	Ru-121 50.1ms	Ru-122 37.2ms	Ru-123 33.7ms	Ru-124 25.1ms	Ru-125 ?	Ru-126 ?	Ru-127 ?	Ru-128 ?		
43	Tc-120 27.0ms	Tc-121 20.5ms	Tc-122 ?	Tc-123 ?	Tc-124 ?	Tc-125 ?	Tc-126 ?			

BACKGOUND

MR Mumpower, Prog. Part. Nucl. Phys. 86 (2016) 86-126

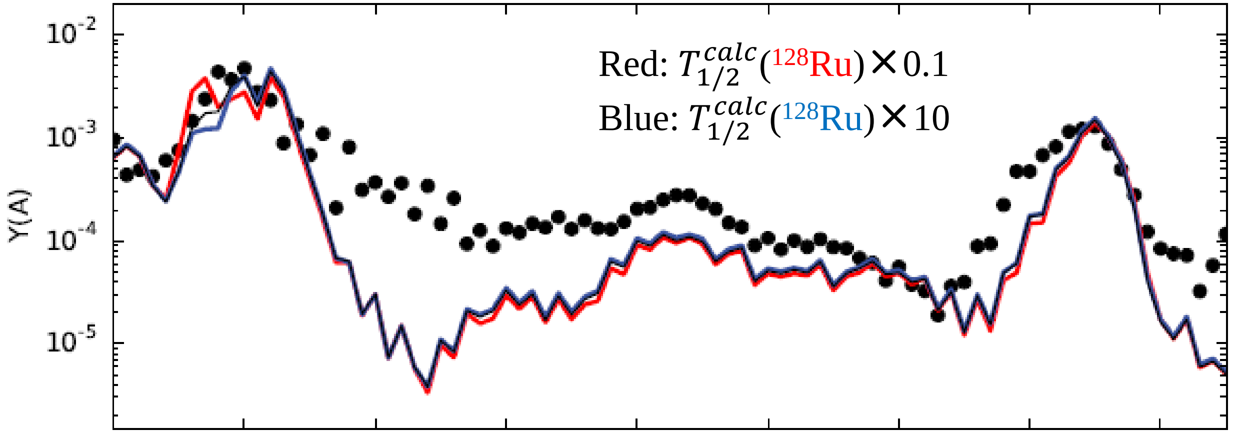
r-process r-abundance pattern

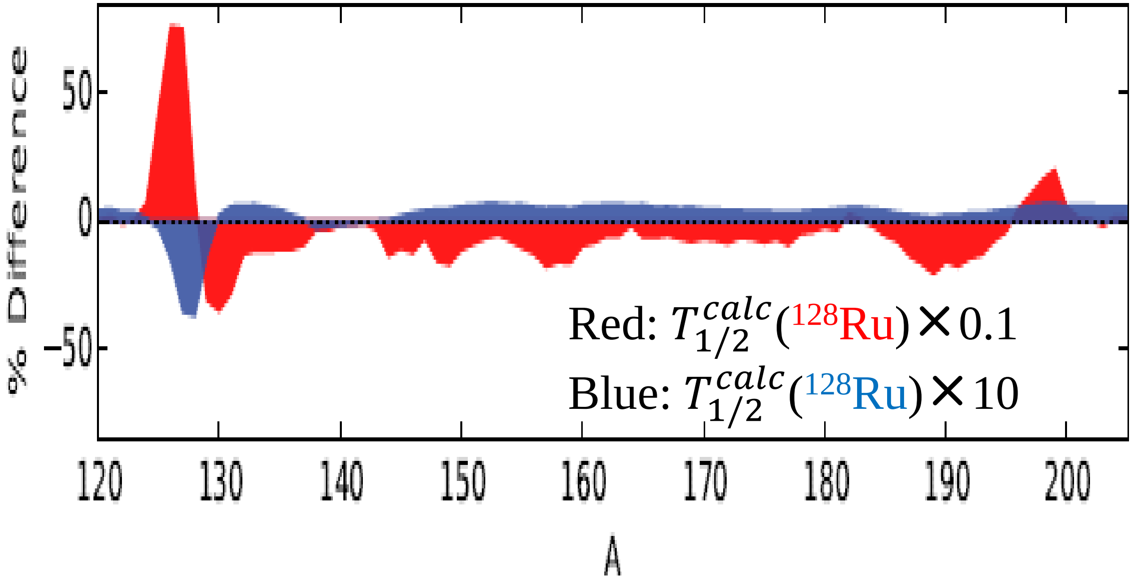
Variation of r-abundance pattern

Unmeasured half-lives give large uncertainties in r-process abundance

Unmeasured β-ray spectra, delayed neutron emission/fission

→Nuclear Data, r-process

BACKGOUND

Predicting Half-Life with Nuclear Models

- FRDM+QRPA

P. Möller et al, At. Data Nucl. Data Tables**66**, 131 (1997).
P. Möller et al, Atomic Data and Nuclear Data Tables 125, 1 (2018).

- HFB+QRPA/FAM

T. Marketin et al, PRC**93**, 025805 (2016).
I. N. Borzov, Phys. At. Nucl. **83**, 700 (2020).
M. Martini et al, PRC **89**, 044306 (2014).
M.T. Mustonen et al, PRC **93**, 014304 (2016), Ney et al, PRC **102**, 034326 (2020).
K. Yoshida Phys. Rev. C **100**, 024316 (2019)

- Gross Theory

T. Yoshida, T. Tachibana, JNST**37**, 491 (2000).
T. Tachibana, RIKEN Review, **26**, 109 (2000).

- Configuration Interaction (CI)

T. Suzuki et al, PRC**85**, 015802 (2012).
Astrophys. J. **859**, 133 (2018).
A. Kumar et al, PRC **109**, 064319 (2024).

- Interacting Boson Model

K. Nomura et al, PRC **101**, 044318 (2020).

- Systematics

K.-L. Kratz, G. Herrmann, Z. Phys., 263 (1973), 435

Predicting Delayed-Neutron/Fission with Nuclear Models

- Cutoff approximation by threshold energy

T. Marketin et al, PRC**93**, 025805 (2016).
P. Möller et al, At. Data Nucl. Data Tables **66**, 131 (1997).
I. N. Borzov, PRC **71**, 065801 (2005).
J-U. Nabi et al, EPJA **52**, 5 (2016).

- Hauser-Feshbach Statistical Model (HFSM)

P. Möller et al, At. Data Nucl. Data Tables **125**, 1 (2019).
M. Mumpower et al, PRC **106**, 065805 (2022)

- Systematics

E.A. McCutchan et al, PRC **86**, 041305(R) (2012).
K. Miernik et al, PRC **88**, 041301(R) (2013).

Feature of the HFB+QRPA+HFSM model

(1) Computationally fast and applicable to all nuclei in the nuclear chart

(2) Have been applied to many studies

FM, T.Marketin, N.Paar, PRC**104**, 044321 (2021)
FM, ZM Niu, HZ.Liang, PRC**106**, 024306 (2022)

Skyrme Hartree-Fock-Bogoliubov (SHFB)

HFB Equation

$$\begin{pmatrix} h-\lambda & \Delta \\ \Delta & -h+\lambda \end{pmatrix}\begin{pmatrix} U \\ V \end{pmatrix} = E\begin{pmatrix} U \\ V \end{pmatrix}$$

h : Kinetic Energy + Mean Field
Δ : Pairing Field
U & V : HFB Wave Function
λ : Fermi Energy

HFB can treat the mean-field and pairing field on equal footing
(HFBCS treats pairings in a perturbative way (independently) on top of HF)

Matrix Element of Pairing Field

$$\Delta_{ij} = \Delta_{T=0,ij} + \Delta_{T=1,ij}$$

Isoscalar

$$|T=0\rangle = \frac{1}{\sqrt{2}}(|pn\rangle - |np\rangle)$$

Isovector

$$|T=1\rangle = \begin{cases} |nn\rangle \\ \frac{1}{\sqrt{2}}(|pn\rangle + |np\rangle) \\ |pp\rangle \end{cases}$$

Shell Structure of ^{130}Cd

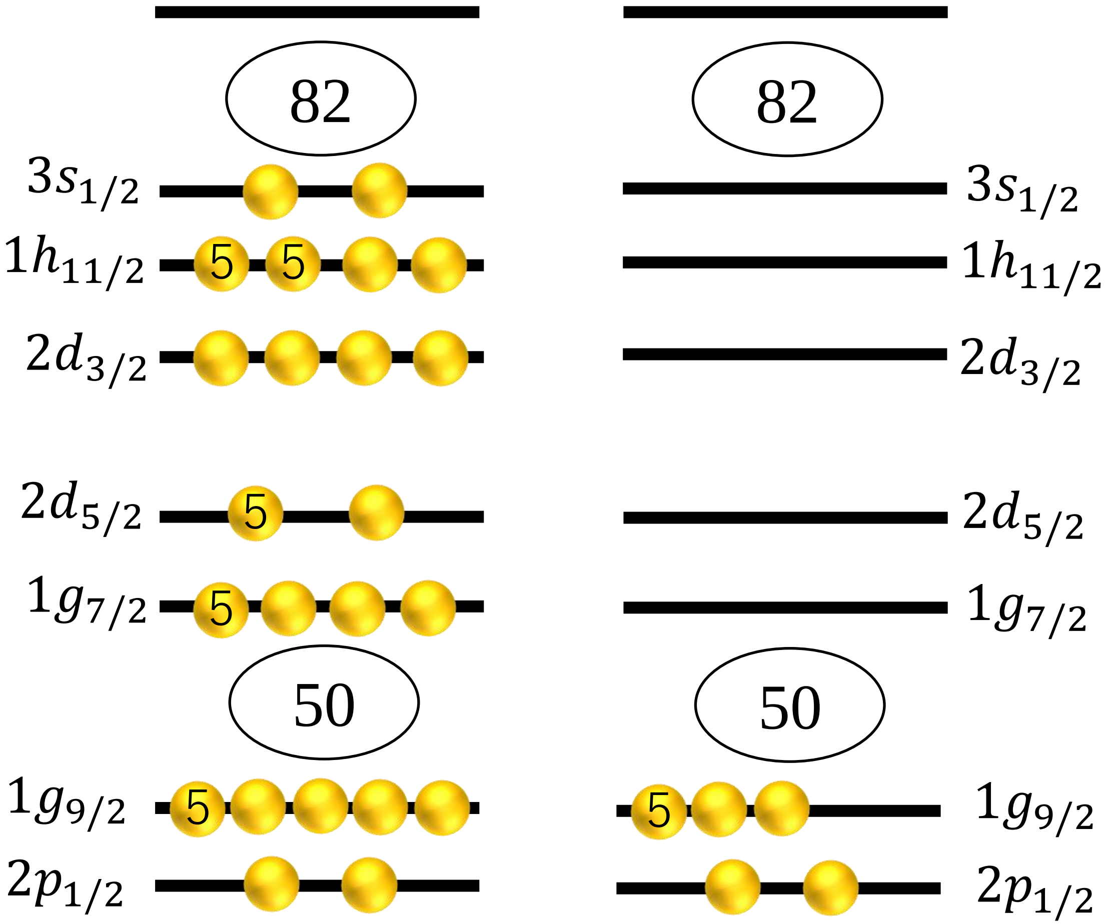

$\Delta_{T=0}$ is neglected due to large difference between *p* & *n* shells

$\Delta_{T=1}$ is determined from an odd-even mass difference (force strength)

Quasiparticle Random Phase Approximation (QRPA)

QRPA phonon creation operator

$$Q^\dagger = \sum_{pn} X_{pn}\psi_p^\dagger\psi_n^\dagger - Y_{pn}\psi_n\psi_p$$

QRPA equation in Canonical Basis

$$\begin{pmatrix} A & B \\ -B & -A \end{pmatrix}\begin{pmatrix} X \\ Y \end{pmatrix} = E_{QRPA}\begin{pmatrix} X \\ Y \end{pmatrix}$$

$$A_{pnp'n'} = \left(E_{pp'}\delta_{nn'} + E_{nn'}\delta_{pp'}\right)$$

2 quasi-particle energy

$$+V_{pnpn}(u_p u_n u_{p'} u_{n'} + v_p v_n v_{p'} v_{n'})$$

particle-particle residual interaction

$$+W_{pnpn}(u_p v_n u_{p'} v_{n'} + v_p u_n v_{p'} u_{n'})$$

particle-hole residual interaction

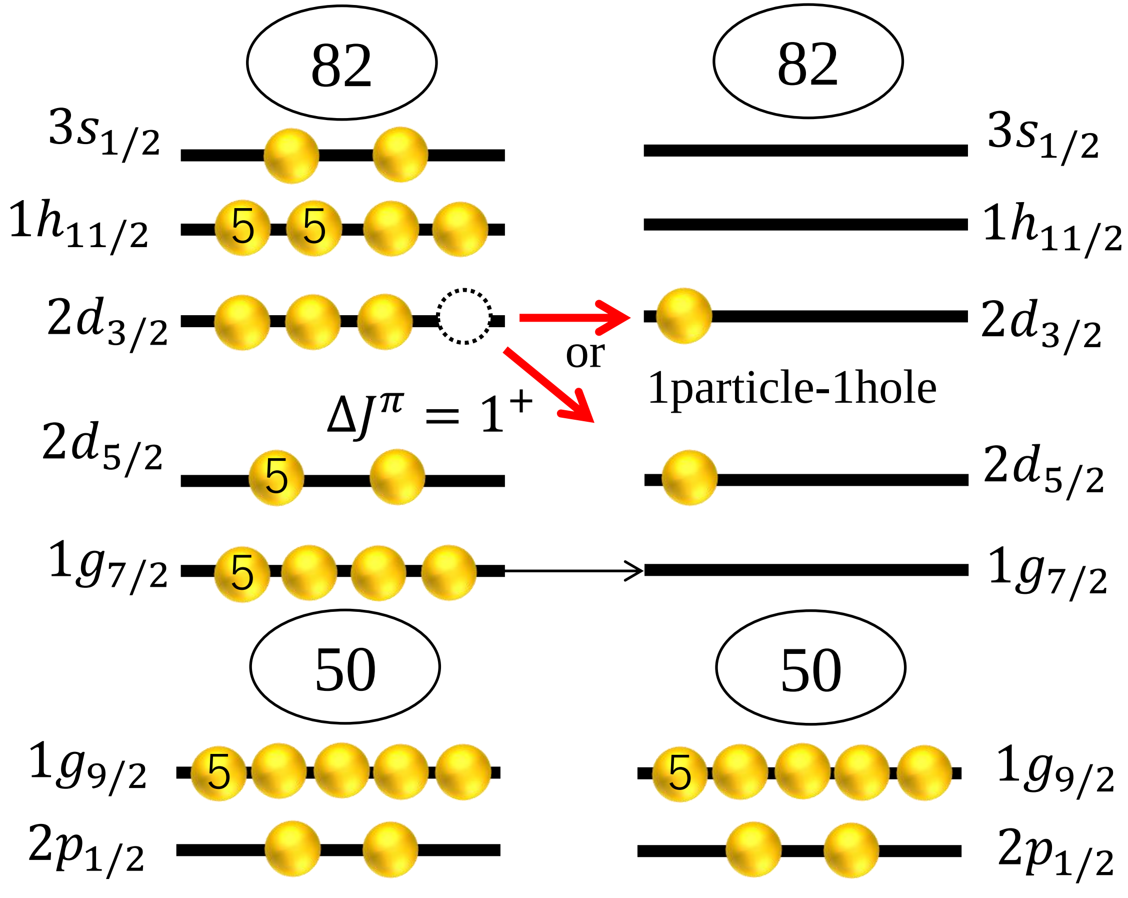

$T = 0$ pairing can be significant in case of excited states, especially of Gamow-Teller States

Pairing correlation in Skyrme HFB+QRPA

Phenomenological pairing force

$$V_{T=1}(r_1,r_2) = f\sum_{i=1}^{2}(W_i + B_iP_\sigma - H_iP_\tau - M_iP_\sigma P_\tau)\, e^{-r_{12}^2/\mu_i^2}$$

Gogny D1S is adopted for $T = 1$ pairing force

f can be determined from odd-even mass difference ($f = 1.0$ in this work)

T=0 pairing correlation has less info than T=1 pairing

T=0 pairing force adopted

$$V_{T=0}(Z,N;r_1,r_2) = V(Z,N)\left(e^{-\mu_1 r_{12}^2} - 2e^{-\mu_2 r_{12}^2}\right)$$

Determine Model Parameter $V(Z,N)$ through expt. data

HFB+QRPA Model Space, Pairing Gap, Half-life for ^{128}Cd

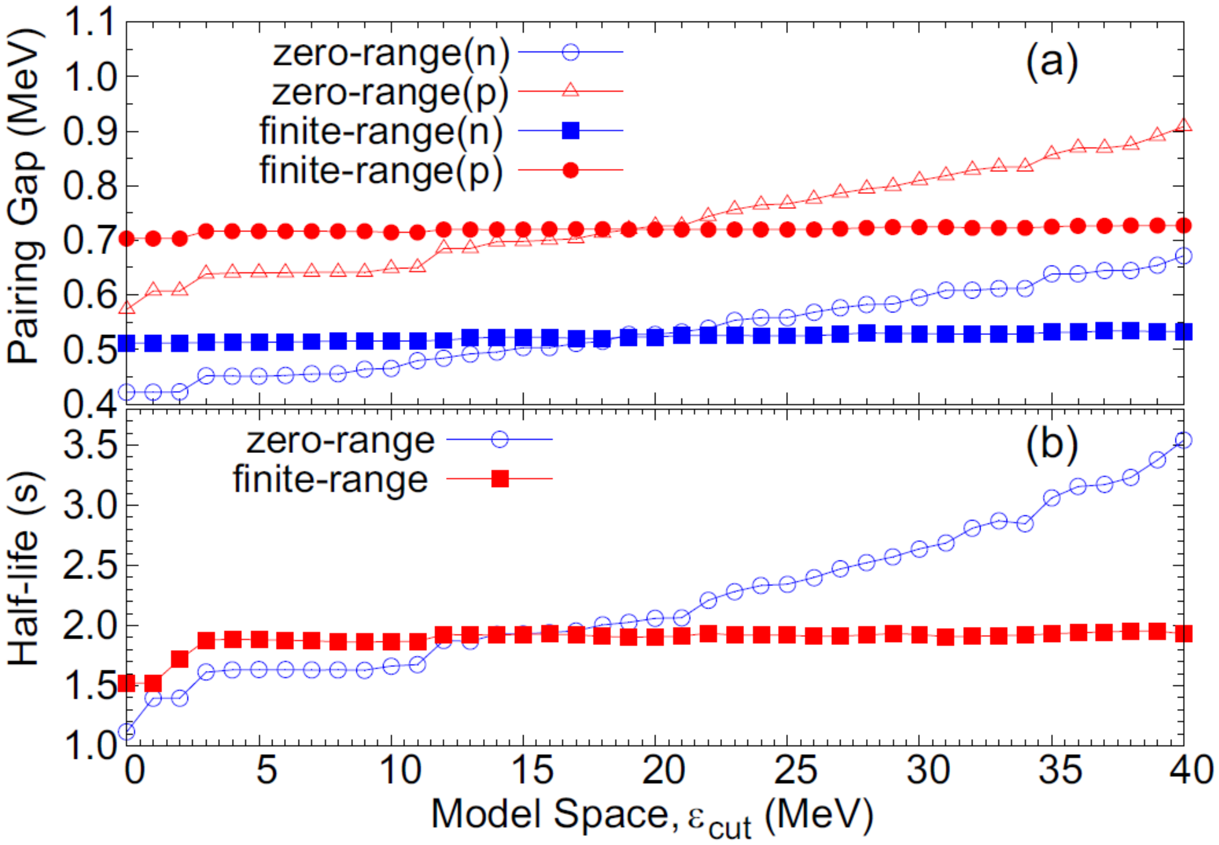

FIG. 2. (a) Average pairing gaps of proton (p) and neutron (n) and (b) β-decay half-life of ^{128}Cd as a function of the cutoff energy $\varepsilon_{\mathrm{cut}}$.

Our STRATEGY

1. Collect $V = V_{opt}$ optimized to $T_{1/2}$ in NUBASE2016 (950 nuclei)
2. Estimate $V(Z, N)$ of neutron-rich nuclei using $V_{opt}(Z, N)$
3. Predict $T_{1/2}$ with the estimated $V(Z, N)$

Bayesian Neutral Network (**BNN**) is used

$$\chi^2 = \sum_{n=1}^{N} \left[\frac{S(\boldsymbol{x};\boldsymbol{\omega}) - V_k}{\Delta V_k} \right]^2 \qquad S(\boldsymbol{x};\boldsymbol{\omega}) = a + \sum_{j=1}^{H} b_j \tanh\left(c_j + \sum_{i=1}^{I} d_{ji} x_i \right)$$

one hidden layer
H=30: number of neurons
I: number of inputs

Model Assumptions

Nuclear Shape

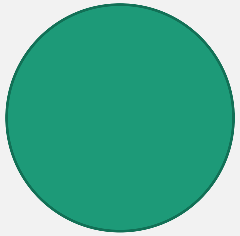

Spherical

Pairing

$|r_1 - r_2| > 0$

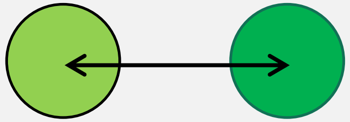

Finite-Range
Pairing Force

Odd Nuclei

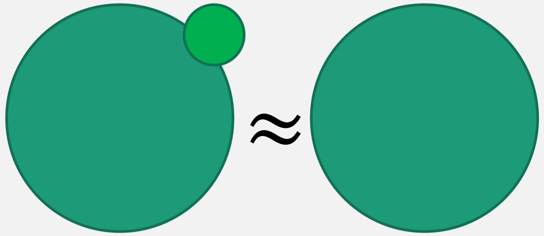

described in the same way
as Even-nuclei

Effective force

SkO'

reproducing
exp Q_β

GT & first-forbidden transitions (0^-, 1^-, 2^-) are included

RESULT

FM, ZM Niu, HZ.Liang, PRC**106**, 024306 (2022)

V_{opt} optimized to $T_{1/2}$ in NUBASE2016

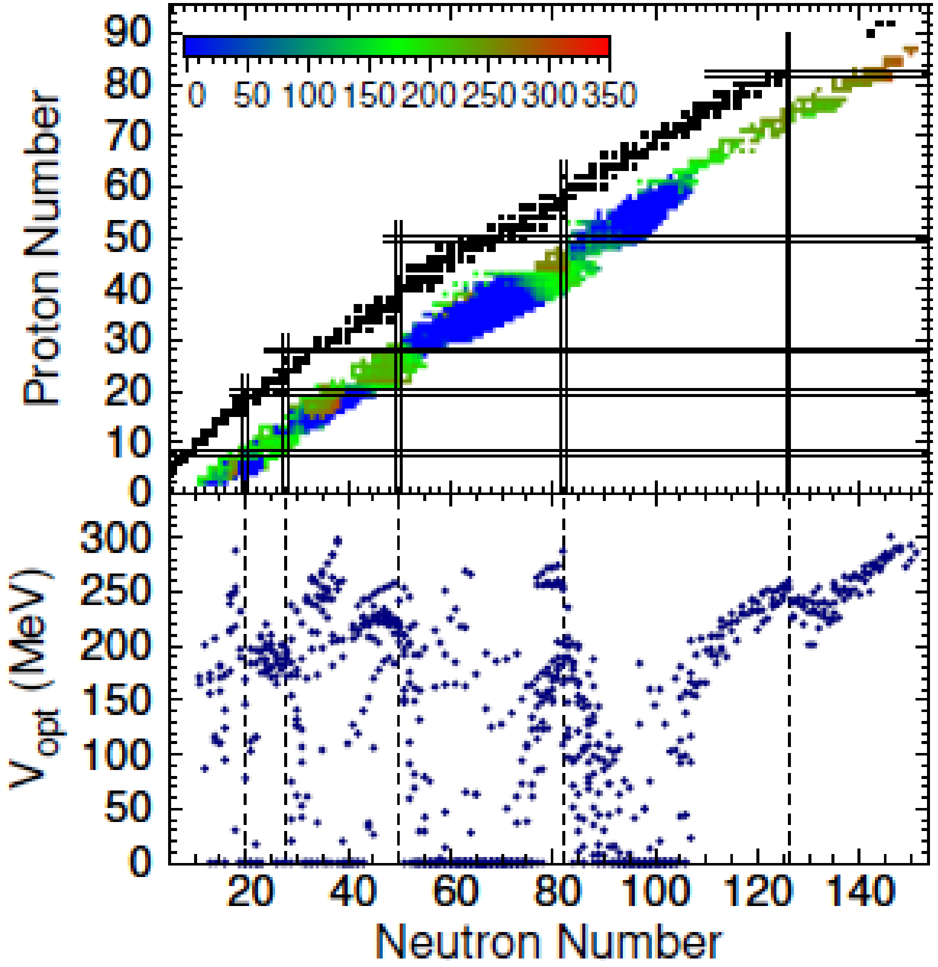

BNN

Result of V_{BNN} learnt from V_{opt} with BNN

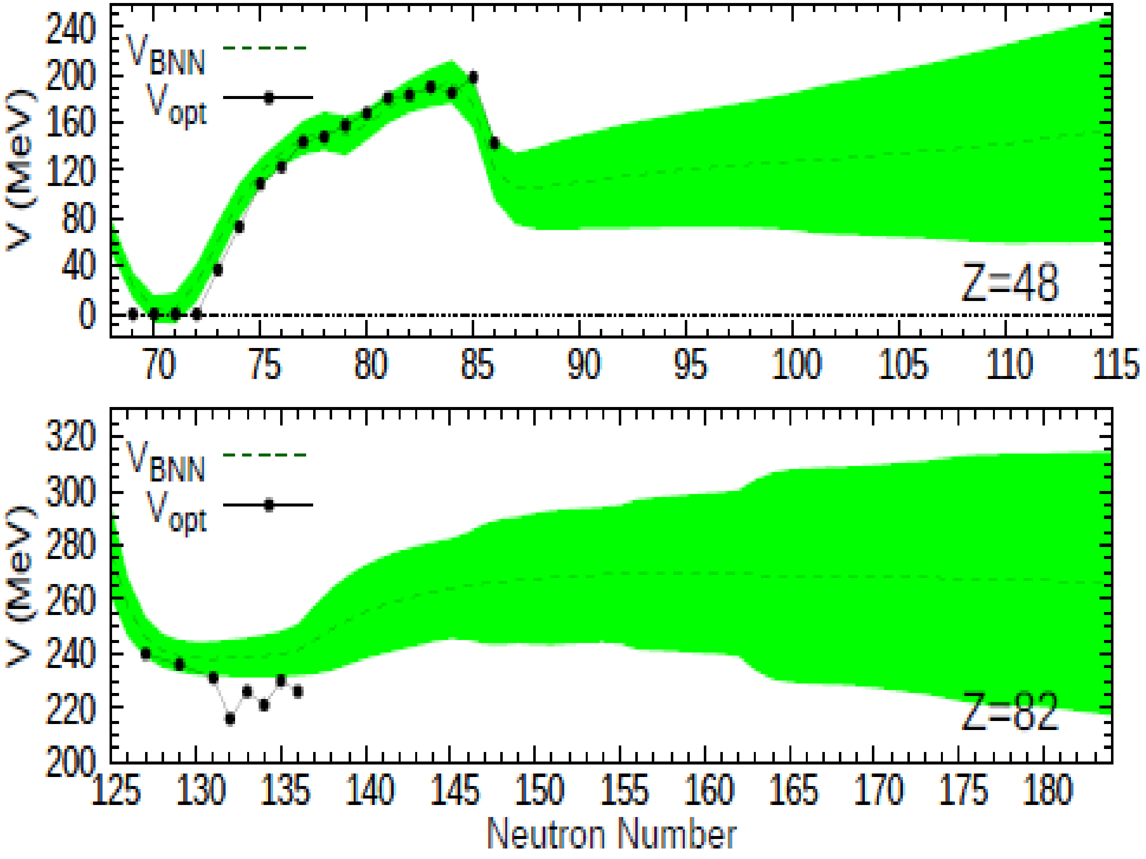

(1) large V_{opt} at magic numbers

(2) $V_{opt} \approx 0$ between magic numbers

$T_{1/2}^{calc}(^{128}\mathrm{Ru})=9.0\pm0.2$ ms

Verifying V_{BNN} for Predictions

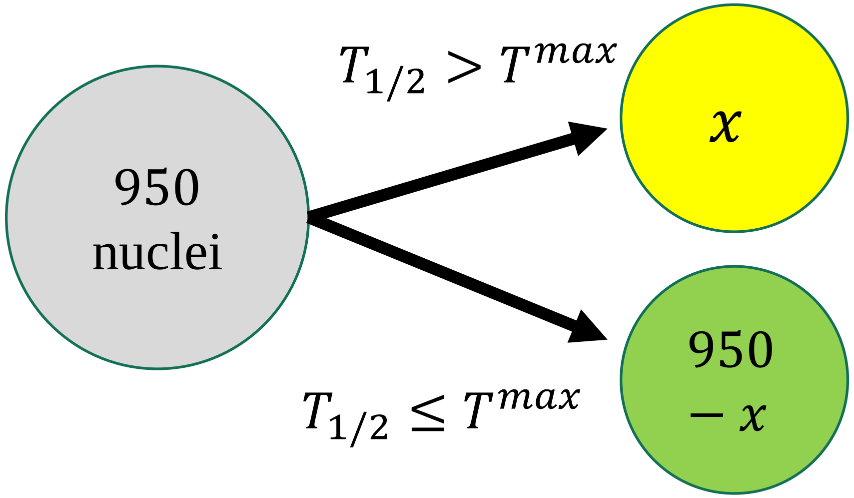

950 nuclei

$T_{1/2} > T^{max}$

x

Training Data of BNN

$T_{1/2} \leq T^{max}$

$950 - x$

Test data of BNN

Mean Deviation $\bar{r} = \frac{1}{N}\sum_i r_i ,$

Standard Deviation $s = \sqrt{\frac{1}{N}\sum_i (r_i - \bar{r})^2}$

Setting	T_{div} (s)	Number of training data, x	Number of test data	$\bar{r}$	s
1	1.00	569	381	−0.080	0.478
2	0.50	626	324	−0.020	0.494
3	0.10	776	174	−0.085	0.335
4	0.05	841	109	−0.031	0.270

$\bar{r} \simeq -0.03$

→7 % underestimation on average

$s \simeq 0.27$

→ within a factor of 1.86

→Expect that V_{BNN} & $T_{1/2}$ are predicted within the same accuracy.

FM, ZM Niu, HZ.Liang, PRC**106**, 024306 (2022)

Deviation from exp $T_{1/2}$

Comparison with exp and other models for Kr, Rb, Cd, In isotopes

950 nuclei

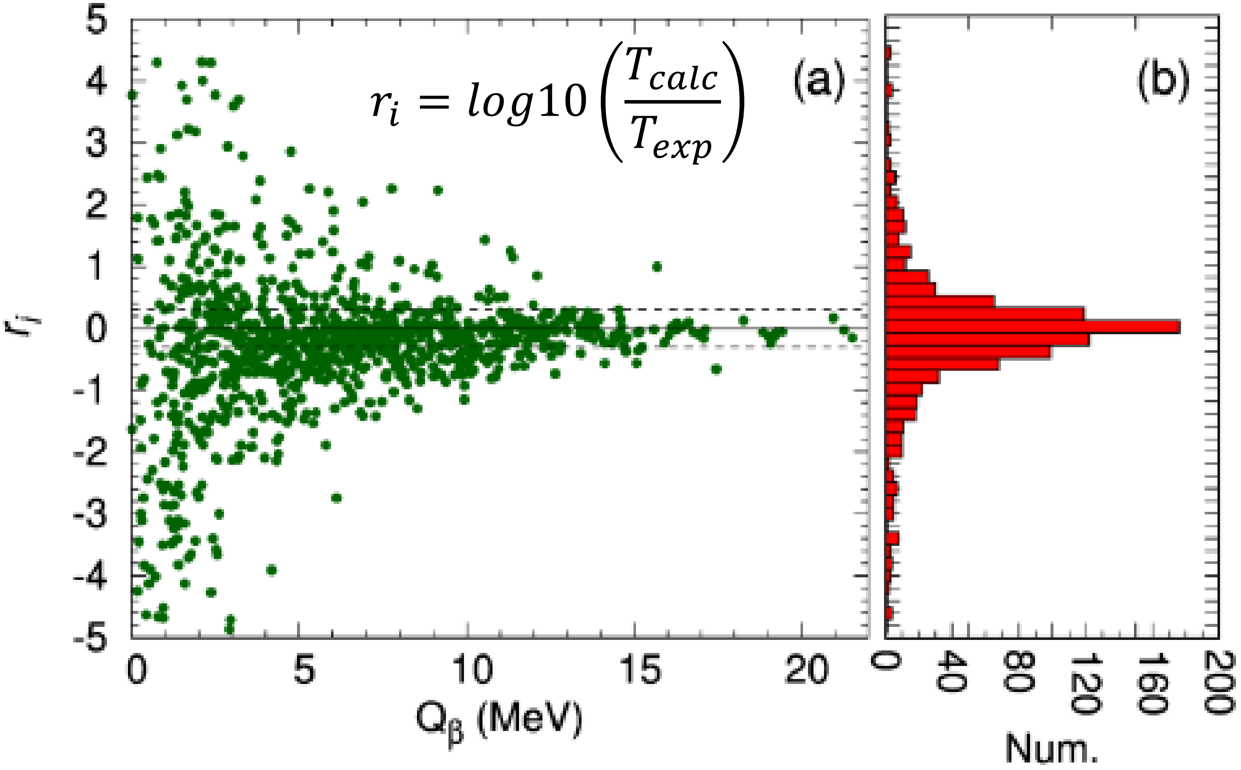

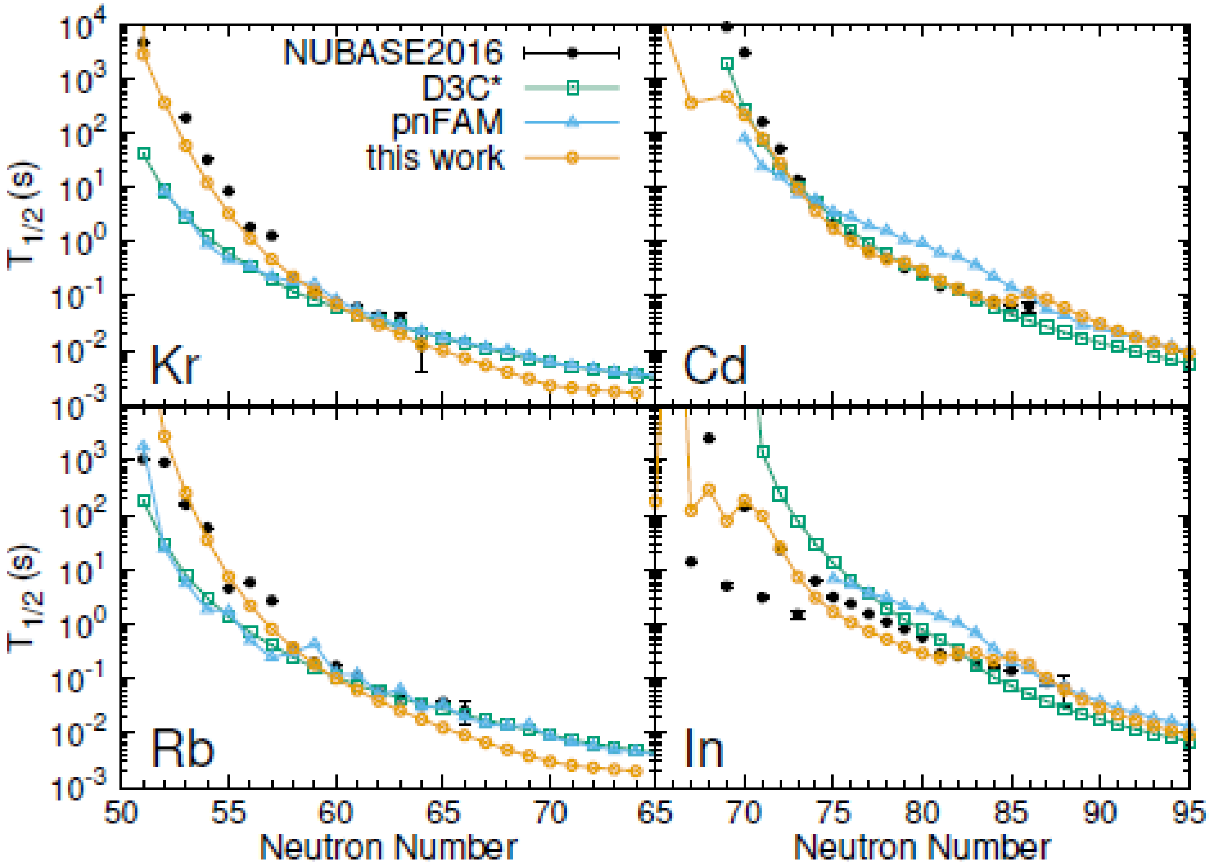

Compare other models by focusing $T_{exp} < 10^3$ s

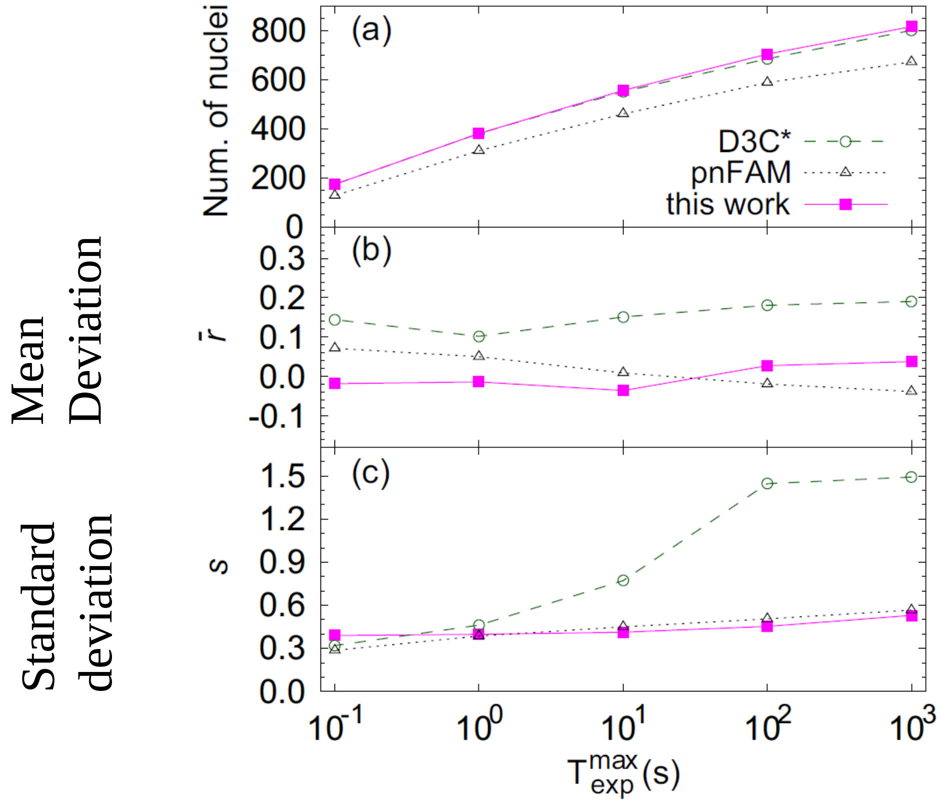

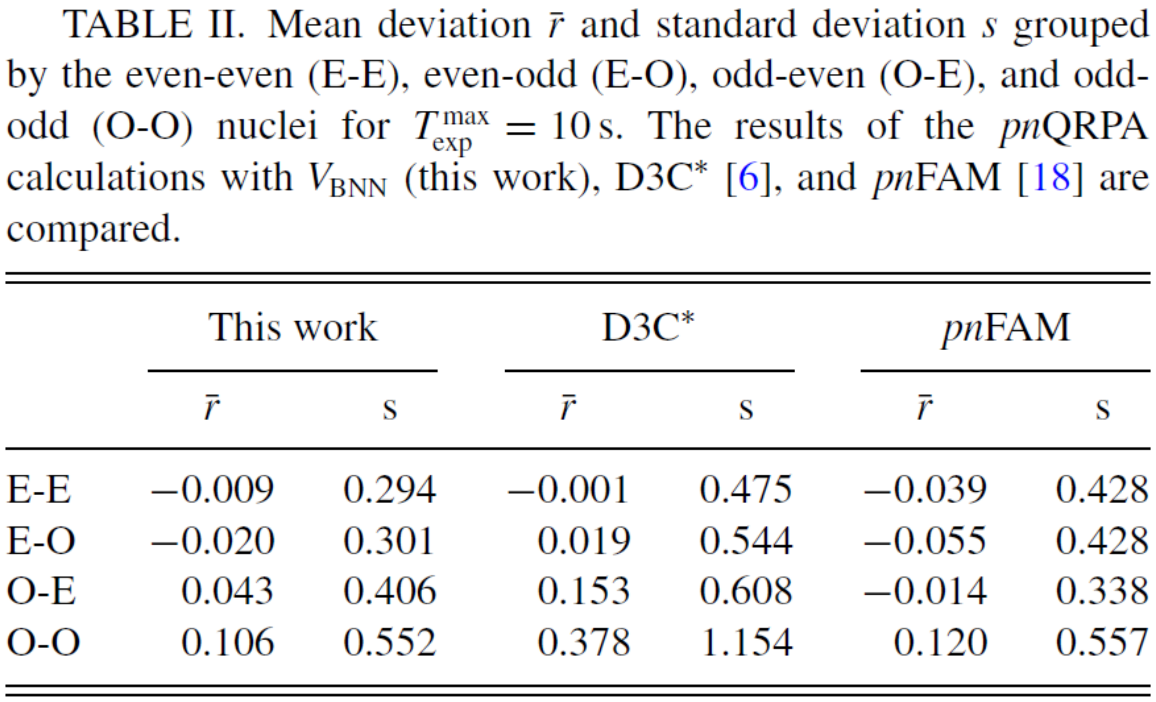

TABLE II. Mean deviation $\bar{r}$ and standard deviation s grouped by the even-even (E-E), even-odd (E-O), odd-even (O-E), and odd-odd (O-O) nuclei for $T_{\mathrm{exp}}^{\mathrm{max}} = 10\,\mathrm{s}$. The results of the *pn*QRPA calculations with V_{BNN} (this work), D3C* [6], and *pn*FAM [18] are compared.

	This work		D3C*		*pn*FAM	
	$\bar{r}$	s	$\bar{r}$	s	$\bar{r}$	s
E-E	−0.009	0.294	−0.001	0.475	−0.039	0.428
E-O	−0.020	0.301	0.019	0.544	−0.055	0.428
O-E	0.043	0.406	0.153	0.608	−0.014	0.338
O-O	0.106	0.552	0.378	1.154	0.120	0.557

D3C*: T. Marketin et al, PRC**93**, 025805 (2016).
pnFAM: Ney et al, PRC **102**, 034326 (2020).

The current result is better than D3C* and comparable to pnFAM

New exp. of RIKEN RIBF measured in 2020

55 data, of which 14 are newly measured

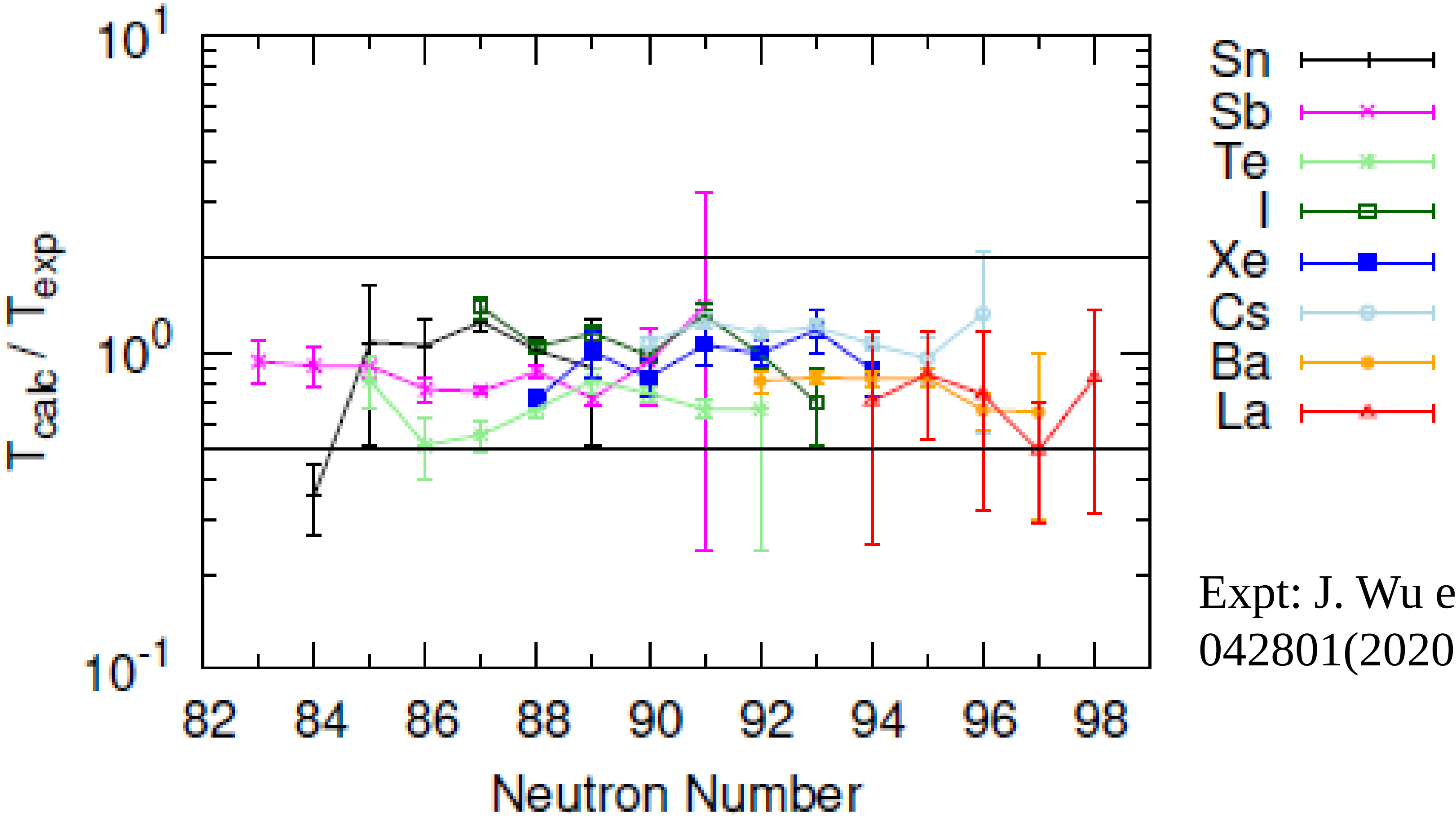

Expt: J. Wu et al. PRC101, 042801(2020)

New exp. $T_{1/2}$ are reproduced within a factor of two

Impact of new expt. data on T=0 pairing strength & half-lives

$$V_{T=0} = V\left(e^{-\mu_1 r_{12}^2} - 2e^{-\mu_2 r_{12}^2}\right)$$

prior BNN: NUBASE2016
new BNN: NUBASE2016+RIKEN2020

edge of available
measured data

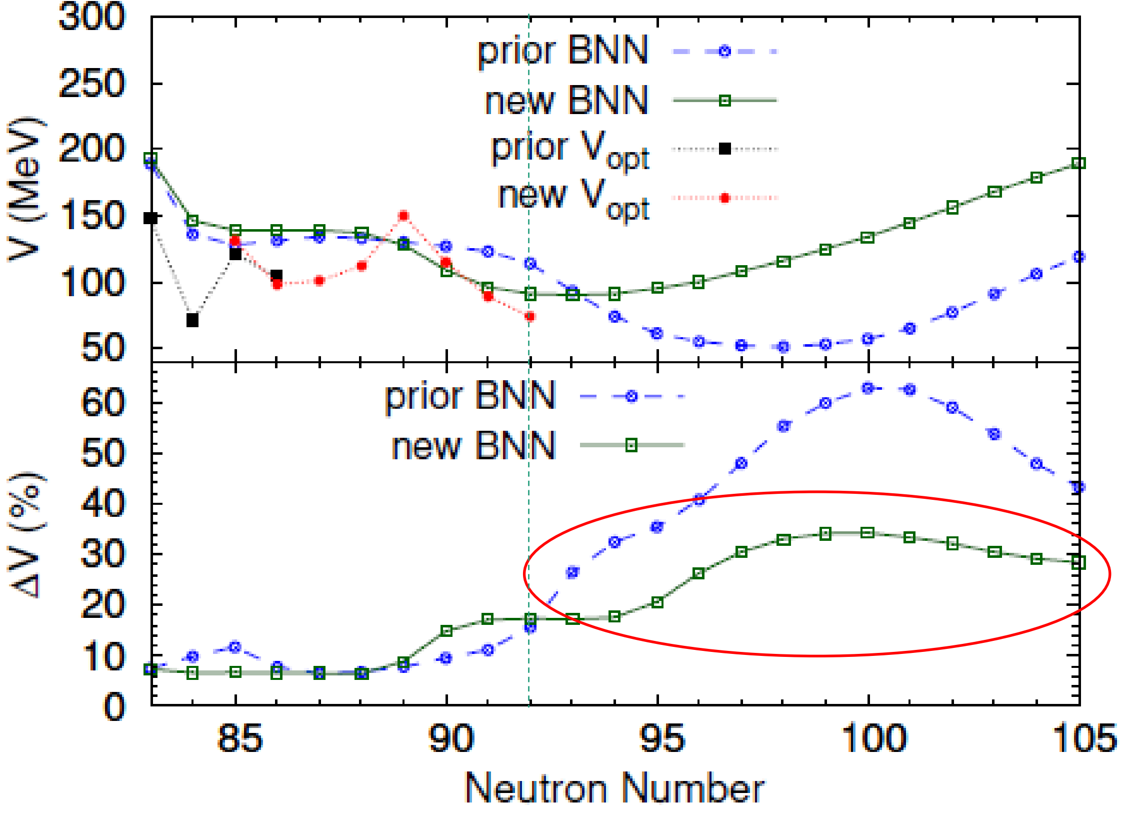

Uncertainty of V is reduced by new exp.

edge of available
measured data

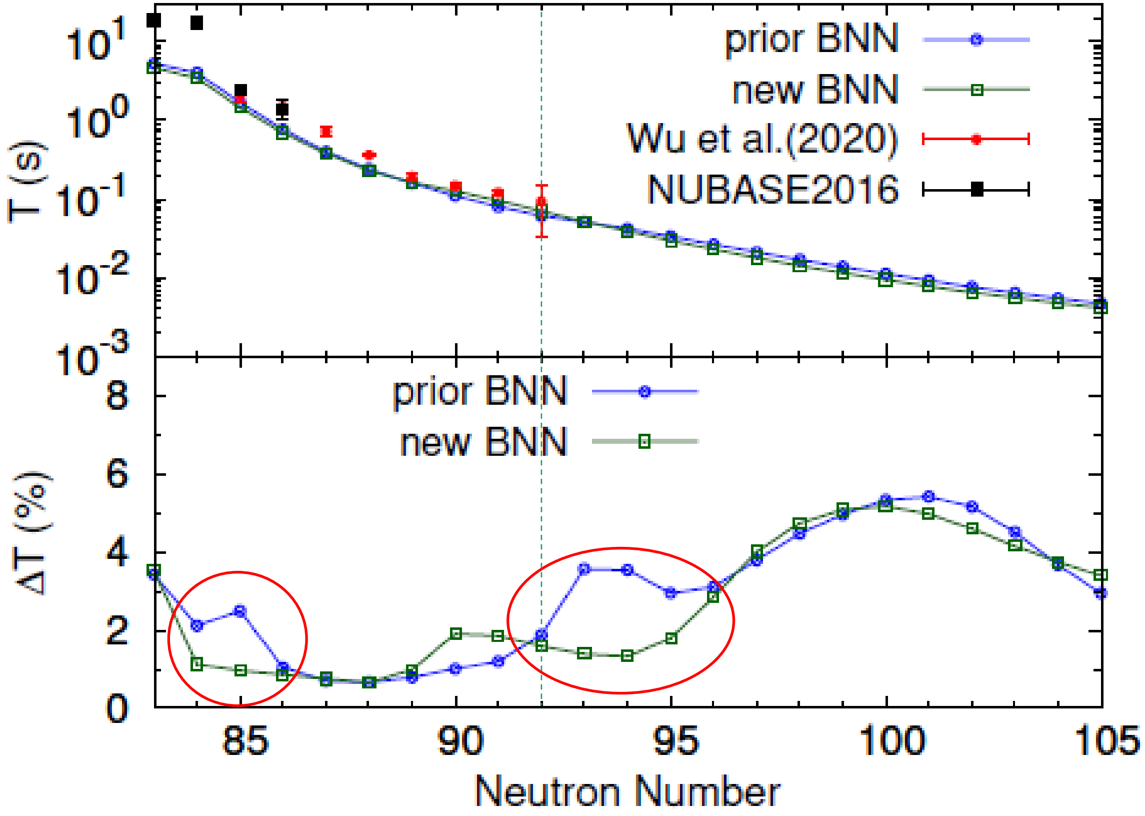

Uncertainty of T is also reduced

r-process simulation

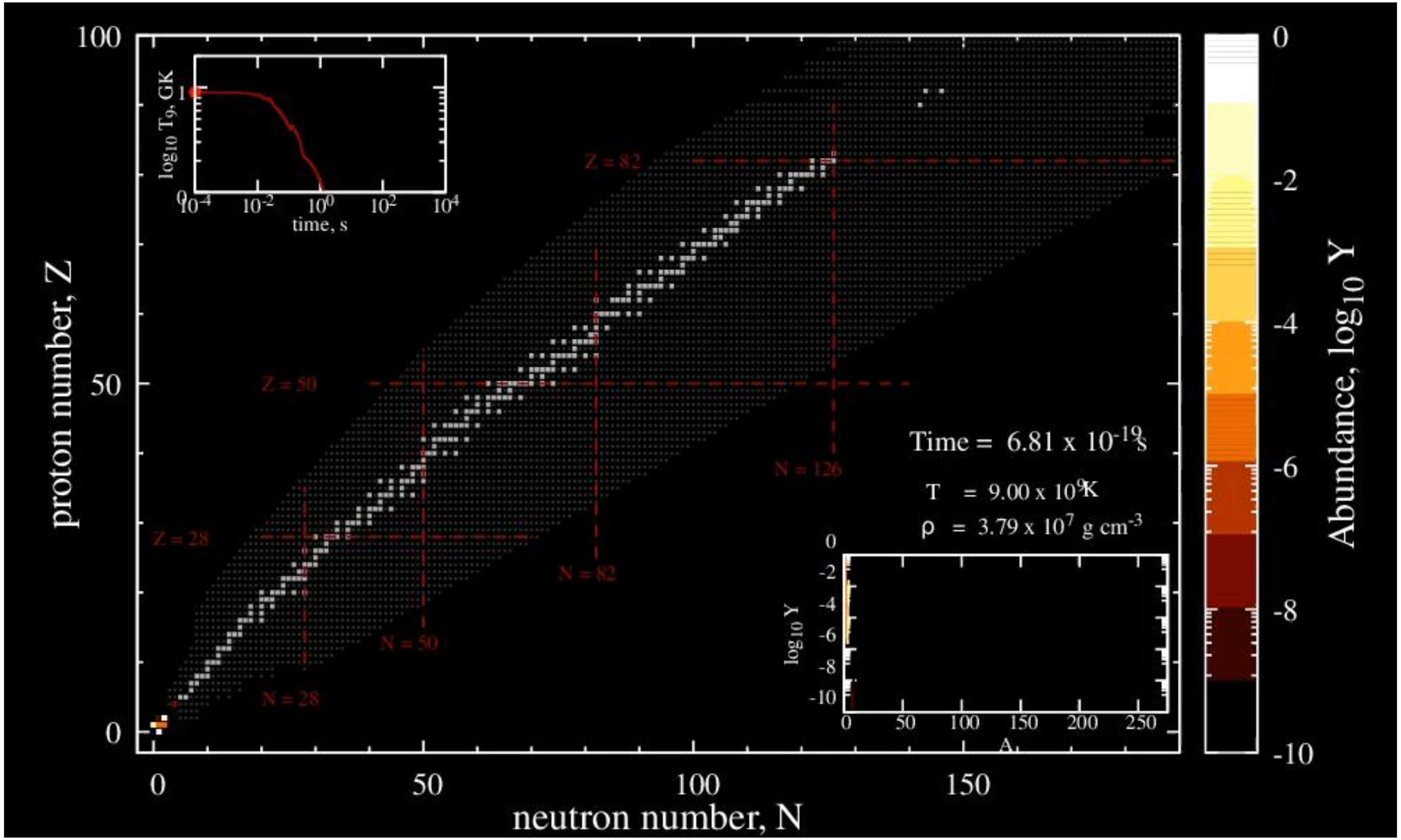

Courtesy of N. Nishimura

Theoretically the shortest half-lives?

pnRQRPA (D3C*) $^{321}_{105}\mathrm{Db}$ $T_{1/2} = 3.5\ \mu\mathrm{s}$

FRDM+QRPA $^{44}_{11}\mathrm{Na}$ $T_{1/2} = 150\ \mu\mathrm{s}$

GT2 $^{247}_{73}\mathrm{Ta}$ $T_{1/2} = 259\ \mu\mathrm{s}$

pnQRPA (SkO') $^{55}_{15}\mathrm{P}$ $T_{1/2} = 584\ \mu\mathrm{s}$

pnFAM (SkO') $^{110}_{33}\mathrm{As}$ $T_{1/2} = 1395\ \mu\mathrm{s}$

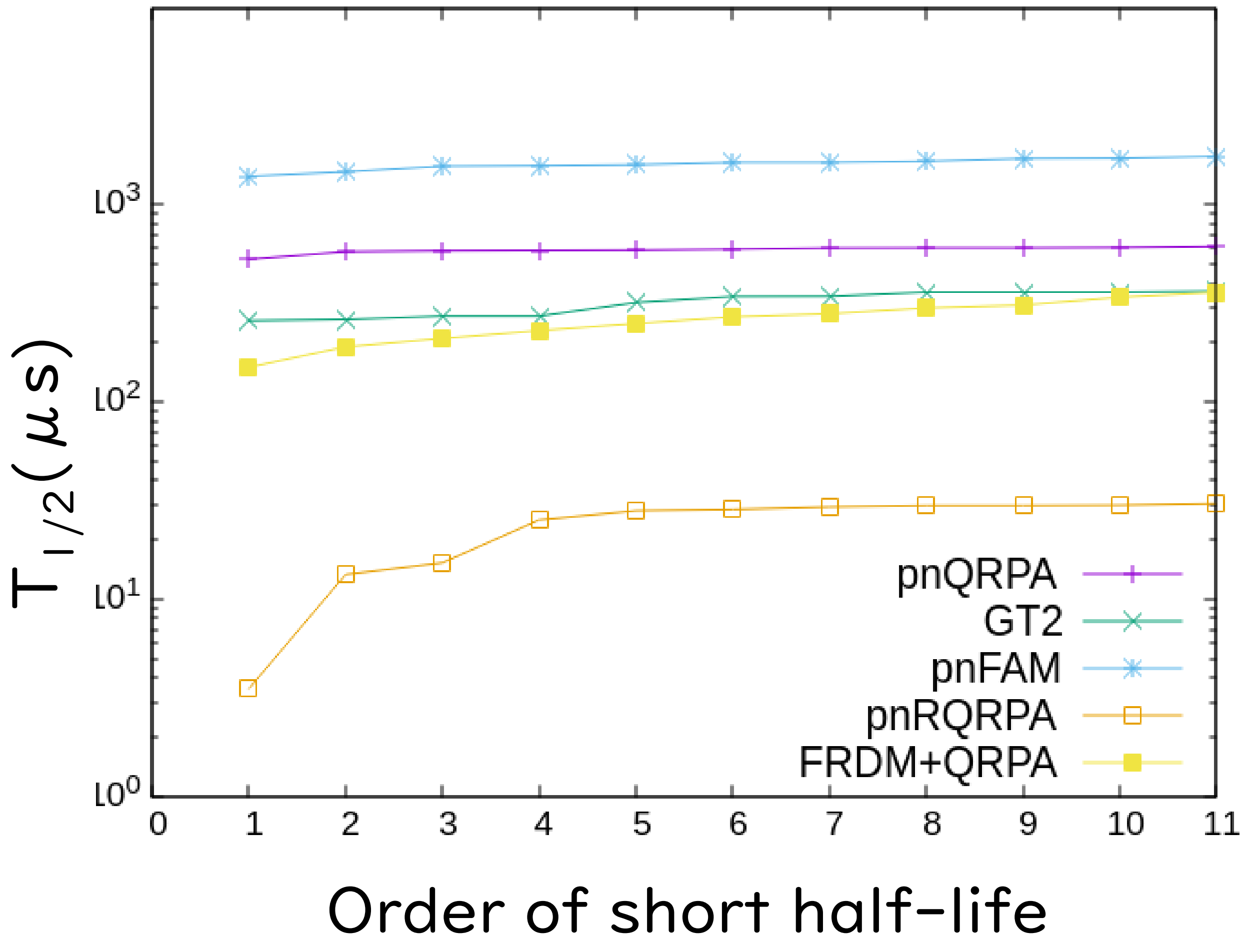

Kratz-Hermann formula

$T_{1/2} \sim a(Q_\beta - C)^{-b}$

Relation between $T_{1/2}$ and Q_β

Kratz-Hermann formula
K.-L. Kratz, G. Herrmann, Z. Phys., 263 (1973), p. 435

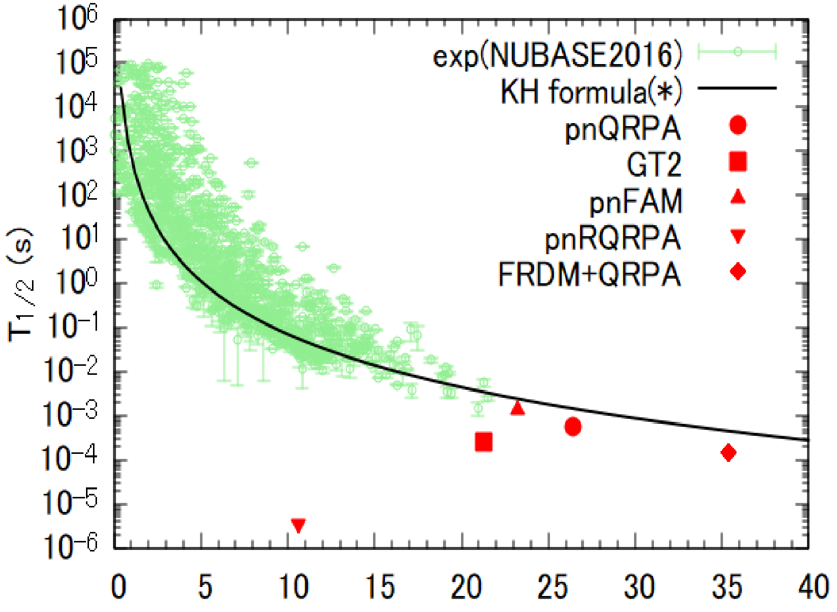

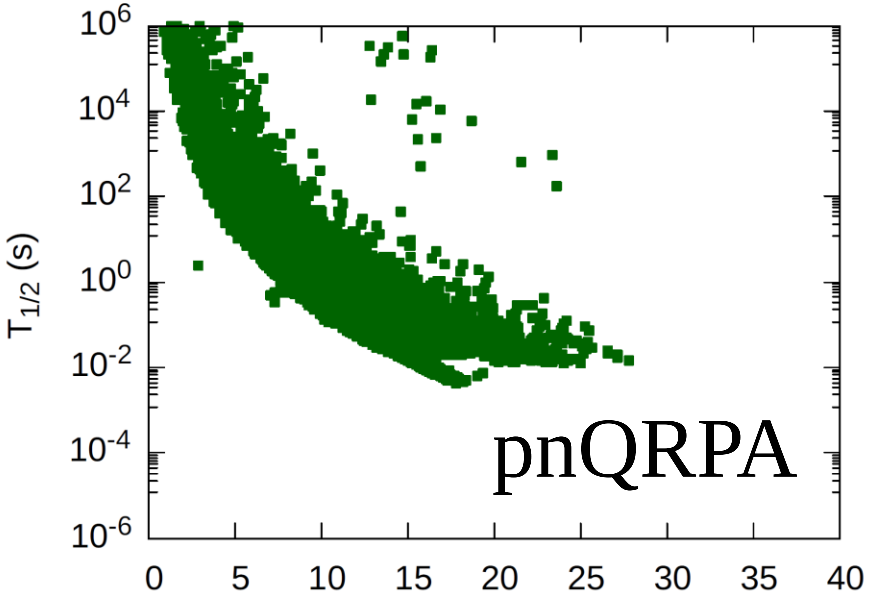

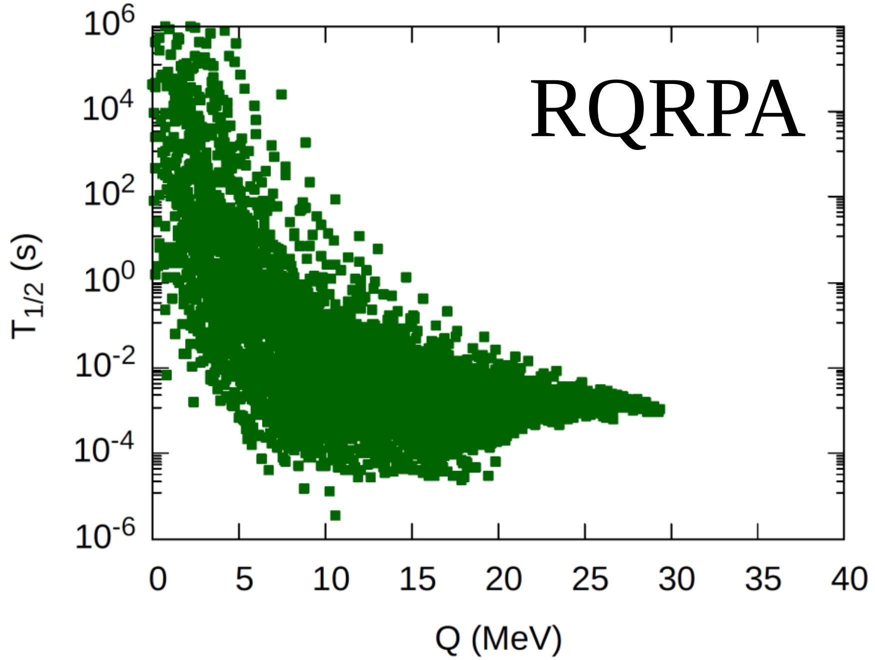

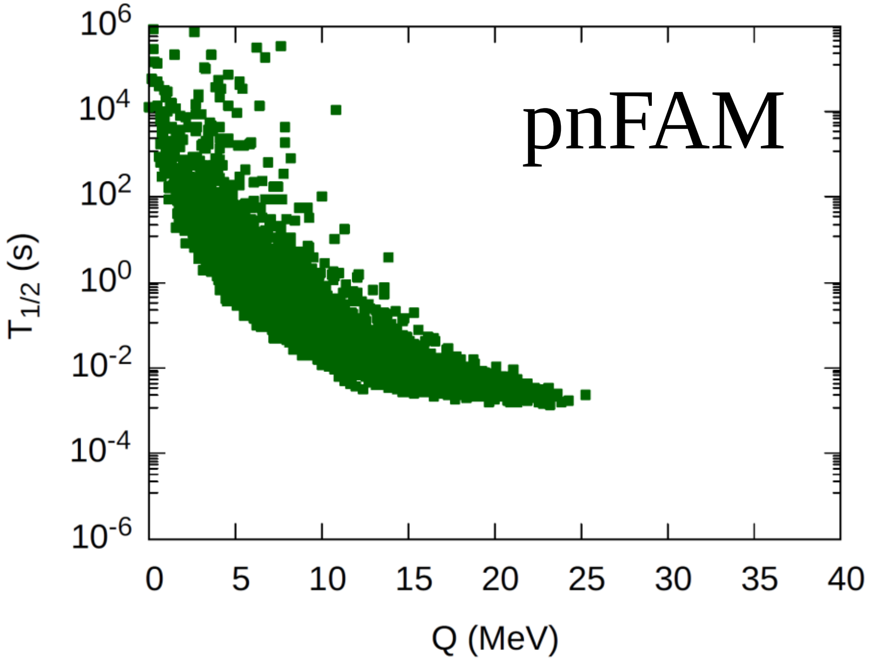

Delayed neutron branching ratios within QRPA+HFSM

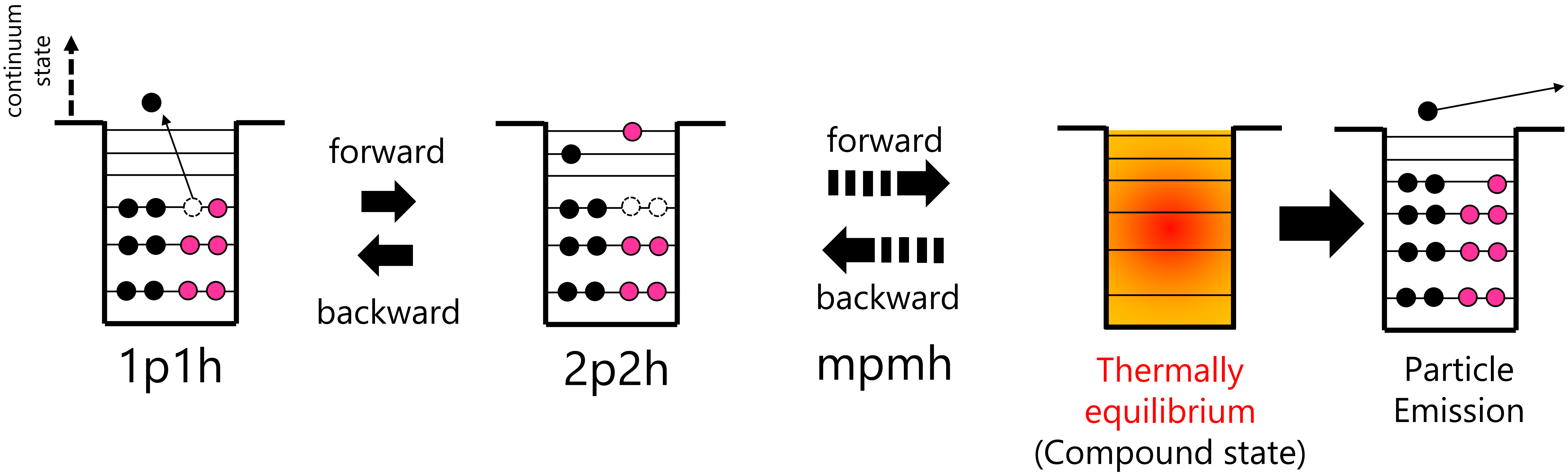

continuum state

1p1h

forward

backward

2p2h

forward

backward

mpmh

Thermally equilibrium
(Compound state)

Particle Emission

HFSM

Delayed neutron branching ratios within QRPA+HFSM

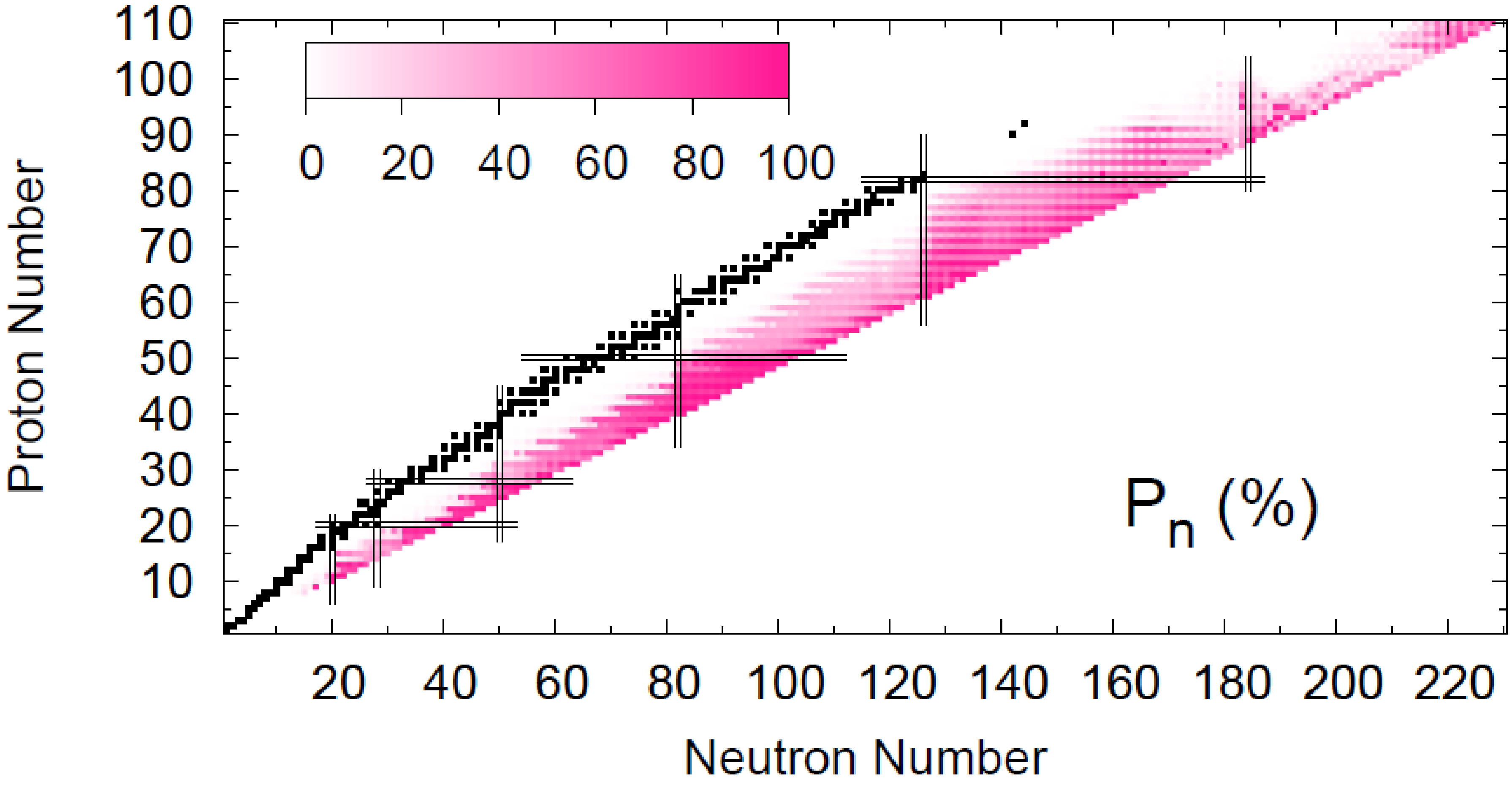

Delayed fission branching ratios within QRPA+HFSM

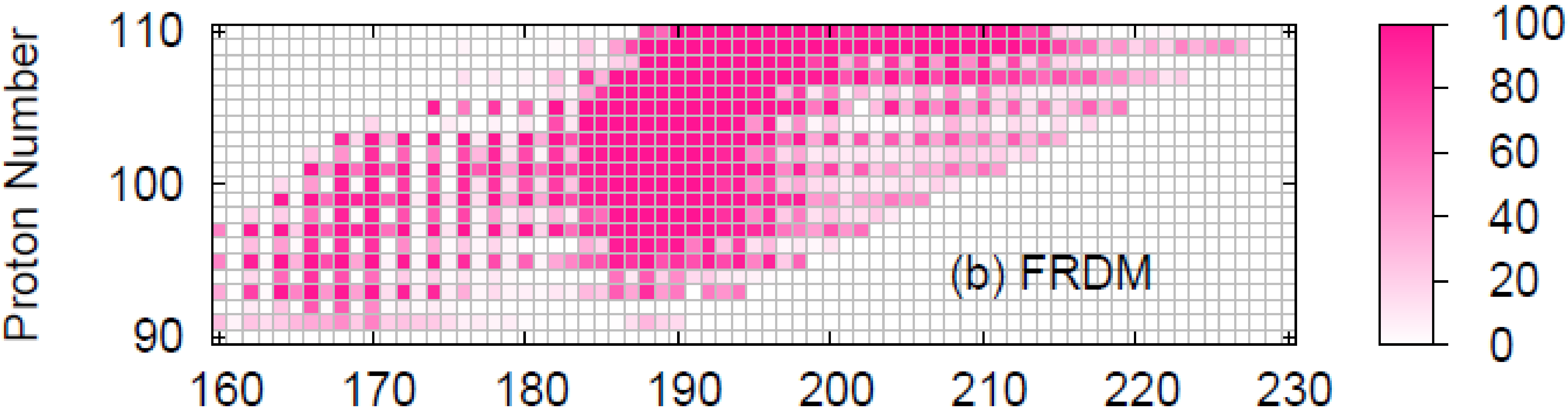

Theoretically, nuclei that emit delayed-neutrons the most?

pnRQRPA (D3C*)+HFSM

$$^{128}_{37}\mathrm{Rb} \quad \langle n \rangle = 8.144$$

FRDM+QRPA

$$^{111}_{28}\mathrm{Ni}\ etc. \quad \langle n \rangle = 10$$

P. Moller et al, Atomic Data Nucl. Data Tables 125,1(2018)

Summary

Predict $T_{1/2}$ by isoscalar pairing predicted by BNN

- ✓Known measured $T_{1/2}$ are reproduced well
- ✓Newly measured $T_{1/2}$ are also reproduced

The result is used for JENDL-5 Decay Data & r-process simulation

Further study is needed for

- ✓Uncertainty of SkO’ effective force
- ✓Impact of P_{2n} (not P_{1n}) on r-process
- ✓Particle emission from direct or preequilibrium process
  Is always compound state true?
- ✓Deformation Effect

Fig: $r_i = log10\left(\frac{T_{calc}}{T_{exp}}\right)$ in the N-Z plane

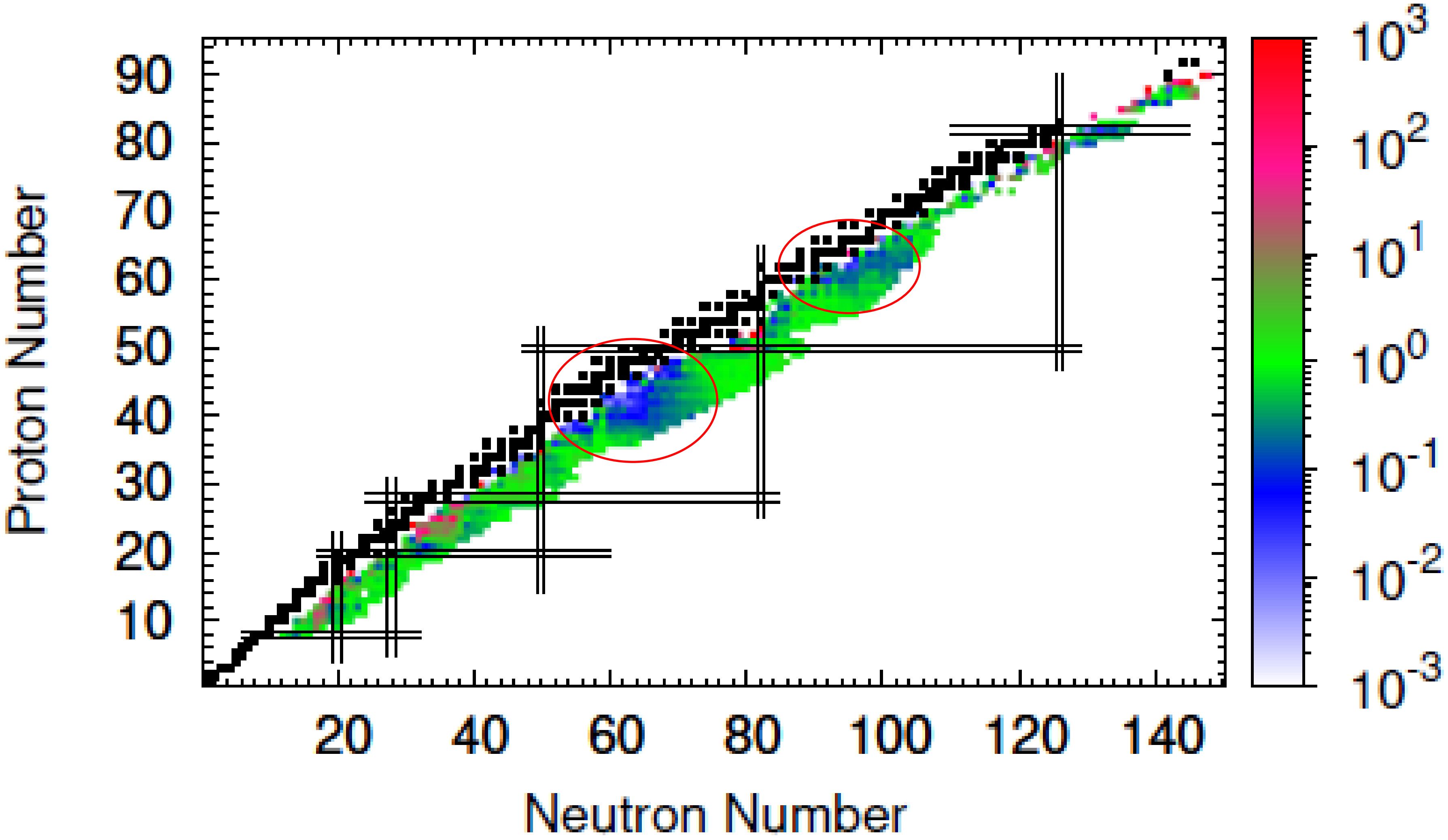

Fig: Comparison with exp and other models for Mo(Z=42), Tc(Z=43), Sm(Z=62) , Eu(Z=63)

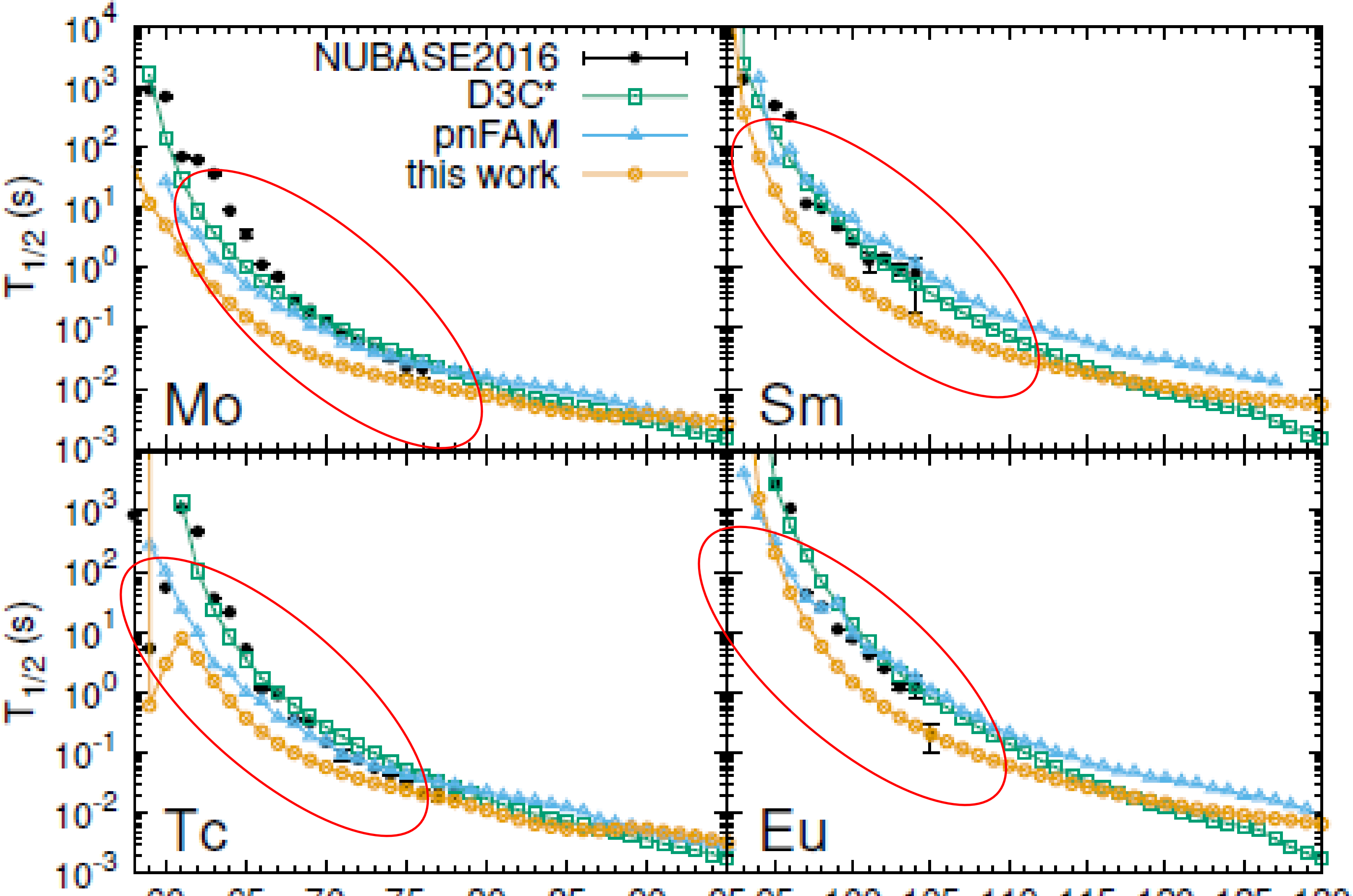

Underestimations arising from spherical shape assumption